

# Mass transfer during low mass X-ray transient decays

Craig R. Powell<sup>1,2\*</sup>, Carole A. Haswell<sup>1\*</sup>, and Maurizio Falanga<sup>3</sup>

<sup>1</sup>*Department of Physics and Astronomy, The Open University, Walton Hall, Milton Keynes MK7 6AA*

<sup>2</sup>*School of Physics and Astronomy, The University of Manchester, Manchester M13 9PL*

<sup>3</sup>*Service d'Astrophysique, DAPNIA/DSM/CEA, 91191 Gif-sur-Yvette, France*

in original form 2006 April 13

## ABSTRACT

The outbursts of low mass X-ray binaries are prolonged relative to those of dwarf nova cataclysmic variables as a consequence of X-ray irradiation of the disc. We show that the time-scale of the decay light curve and its luminosity at a characteristic time are linked to the radius of the accretion disc. Hence a good X-ray light curve permits two independent estimates of the disc radius. In the case of the milli-second pulsars SAX J 1808.4-3658 and XTE J 0929-314 the agreement between these estimates is very strong. Our analysis allows new determinations of distances and accretion disc radii. Our analysis will allow determination of accretion disc radii for sources in external galaxies, and hence constrain system parameters where other observational techniques are not possible. We also use the X-ray light curves to estimate the mass transfer rate. The broken exponential decay observed in the 2002 outburst of SAX J 1808.4-3658 may be caused by the changing self-shadowing of the disc.

**Key words:** accretion, accretion discs, binaries: close, x-rays: binaries, stars: individual: XTE J 1808.4-3658, stars: individual: 4U 1705-44

## 1 INTRODUCTION

King & Ritter (1998) (henceforth KR) and Shahbaz, Charles & King (1998) (henceforth SCK) examined the X-ray light curves of transient low mass X-ray binaries (LMXBs) in decay, characterising them as simple exponential or linear decays. In some cases, however, the decays show a distinct knee. As shown in Fig. 2, this is not a secondary maximum in the sense that the X-ray count rate declines throughout.

In X-ray bright disc-accreting systems, including transient LMXBs during outburst, the temperature of the accretion disc is dominated by X-ray heating from the inner accretion regions across most of the disc. For a disc in which the scale height can be described as a function of radius by  $H = H_0 R^n$  for constant  $H_0$  and  $n$ , the temperature,  $T$ , is given by de Jong, van Paradijs & Augusteijn (1996) as

$$T^4 = \frac{1 - \mathcal{A}}{4\pi\sigma R^2} \frac{H}{R} (n - 1) L_X, \quad (1)$$

where  $\mathcal{A}$  is the disc albedo,  $L_X$  is the central X-ray luminosity heating the disc, assumed to be emanating radially from a small spherical source. Only if  $n > 1$  is the whole surface of the accretion disc illuminated; if  $n = 1$  (1) predicts a surface temperature of zero which is invalid because of local viscous heat production. Consistent with KR we adopt a value of

$n = 9/7$ , although see section 5. (1) can be rewritten to give the maximum radius  $R_h$  which is heated by X-rays to the temperature  $T_h$  needed to remain in the hot, viscous state. Thus

$$R_h^{3-n} = \frac{1 - \mathcal{A}}{4\pi\sigma T_h^4} H_0 (n - 1) L_X. \quad (2)$$

We abbreviate this equation as

$$R_h^{3-n} = \Phi L_X. \quad (3)$$

We note that especially in the case of a black hole the X-ray source will be the inner accretion disc, and as such disc-like rather than point-like. This introduces a factor of  $H/R$  into the r.h.s. of (2), which is equivalent to modified values of  $n$  and  $\Phi$  in (3); specifically, the index of  $3 - n$  in the l.h.s. becomes  $4 - 2n$ , and  $\Phi$  gains a factor of  $H_0$ . However,  $n$  and  $H_0$  may differ systematically between neutron star and black hole systems, in which case the differences in (3) will be less simple.

KR showed that X-ray heating during the decay from outburst causes the light curves of transient LMXBs to exhibit either exponential or linear declines depending on whether or not the luminosity is sufficient to keep the outer disc edge hot. They note that exponential decays must revert to the linear mode when the X-ray flux has decreased sufficiently, but do not analyse this in detail. Nor do they consider the effects of mass transfer from the donor star,  $-\dot{M}_2$ , during the outburst. Whilst in many systems  $-\dot{M}_2$

\* E-mail: craig.powell@manchester.ac.uk (CRP); c.a.haswell@open.ac.uk (CAH)

is negligible compared to the mass accretion rate onto the compact object,  $\dot{M}_c$ , during outburst, this is not necessarily the case. In this paper we consider these issues. Section 2 contains our theoretical predictions for the decay light curve. In section 3 we identify some suitable light curves and describe their parametrization. We compare the results from the fitting in section 4.

## 2 ANALYSIS

### 2.1 Exponential decay

The mass of the accretion disc during the exponential decay is given by equation 3 of KR;

$$M_{\text{disc}} = \frac{\dot{M}_c R_{\text{disc}}^2}{3\nu_{\text{KR}}}, \quad (4)$$

where  $\nu_{\text{KR}}$  is some measure of viscosity, taken by KR to be the viscosity near the outer disc edge with a value of  $\nu_{\text{KR}} \sim 10^{11} \text{ m}^2 \text{ s}^{-1}$ . In the case of significant mass transfer into the disc from the donor star the central accretion rate is given by

$$\dot{M}_c = -\dot{M}_2 - \dot{M}_{\text{disc}}. \quad (5)$$

Using this to replace  $\dot{M}_c$  in (4) we obtain

$$-\dot{M}_2 - \dot{M}_{\text{disc}} = \frac{3\nu_{\text{KR}} \dot{M}_{\text{disc}}}{R_{\text{disc}}^2}. \quad (6)$$

Therefore the mass of the hot disc can be written

$$M_{\text{disc}} = M_\alpha \exp\left(-\frac{3\nu_{\text{KR}} t}{R_{\text{disc}}^2}\right) + \frac{R_{\text{disc}}^2 (-\dot{M}_2)}{3\nu_{\text{KR}}}, \quad (7)$$

where  $M_\alpha$  is the constant of integration, and the X-ray luminosity is proportional to

$$\dot{M}_c = -\dot{M}_2 + \frac{3M_\alpha \nu_{\text{KR}}}{R_{\text{disc}}^2} \exp\left(-\frac{3\nu_{\text{KR}} t}{R_{\text{disc}}^2}\right). \quad (8)$$

At some time,  $t_t$ , the temperature of the outer disc edge, while still dominated by X-ray heating, will be only just sufficient to remain in the hot, viscous state, i.e.  $R_h = R_{\text{disc}}$ . We denote the corresponding X-ray luminosity as  $L_t$ , with the central accretion rate  $\dot{M}_t$ . The X-ray luminosity at earlier times is

$$L_X = (L_t - L_2) \exp\left(-\frac{3\nu_{\text{KR}}(t - t_t)}{R_{\text{disc}}^2}\right) + L_2, \quad (9)$$

where  $L_2 = \eta(-\dot{M}_2)c^2$ , and  $\eta \simeq 0.1$  is the efficiency with which rest mass is liberated as X-rays.

### 2.2 Linear decay

When  $R_h < R_{\text{disc}}$  the outer part of the disc is no longer kept in the hot, viscous state by central irradiation. The radius of the hot part of the disc will decrease with the decreasing X-ray luminosity, corresponding to the late linear decline of KR. This, too, may be modified by the donor star mass loss rate, depending on the mass accretion rate through the now cold outer disc. Designating  $\mu_c(R)$  as the rate at which mass is transported inwards through the cold disc, we examine the two extreme behaviours of  $\mu_c$ . For the minimally efficient cold disc  $\mu_c(R) = 0$  for all  $R$ , and none

of  $-\dot{M}_2$  reaches the hot disc when  $R_h < R_{\text{disc}}$ . At the other extreme  $\mu_c(R) = -\dot{M}_2$  and the cold disc does not increase in surface density with time. The occurrence of outbursts suggests that the latter case is false; with stable cold-state mass transfer, outbursts would never occur.

The mass in the hot disc changes due to three factors: accretion from its inner edge, the loss of material into the encroaching cold disc, and mass transfer from the cold disc. Hence,

$$\dot{M}_{\text{hot}} = -\dot{M}_c + \mu_c(R_h) + 2\pi R_h \Sigma(R_h) \dot{R}_h. \quad (10)$$

Using the approximate substitution from (3) that

$$R_h^2 = \Phi \eta c^2 \dot{M}_c, \quad (11)$$

(10) becomes

$$\dot{M}_{\text{hot}} = -\dot{M}_c + \mu_c(R_h) + \pi \Phi \eta c^2 \Sigma(R_h) \ddot{M}_c. \quad (12)$$

Additionally, equation 2 of KR allows  $M_{\text{hot}}$  to be written as

$$M_{\text{hot}} = \frac{\dot{M}_c R_h^2}{3\nu_{\text{KR}}}. \quad (13)$$

Equating (12) to d/dt (13),

$$\frac{1}{3\nu_{\text{KR}}} \frac{d}{dt} \dot{M}_c R_h^2 = -\dot{M}_c + \mu_c(R_h) + \pi \Phi \eta c^2 \Sigma(R_h) \ddot{M}_c, \quad (14)$$

so using equation 2 of KR,

$$\ddot{M}_c = \frac{3\nu_{\text{KR}}}{\Phi \eta c^2} \left( \frac{\mu_c(R_h)}{\dot{M}_c} - 1 \right). \quad (15)$$

We now substitute the two cases of  $-\mu_c(R_h)$  outlined above. When mass transfer into the hot disc is negligible,

$$\ddot{M}_c = -\frac{3\nu_{\text{KR}}}{\Phi \eta c^2}, \quad (16)$$

and the decay is the linear decline predicted by KR as expected. When  $\mu_c(R_h) = -\dot{M}_2$ ,

$$\ddot{M}_c = \frac{3\nu_{\text{KR}}}{\Phi \eta c^2} \frac{(-\dot{M}_2 - \dot{M}_c)}{\dot{M}_c}. \quad (17)$$

While  $\dot{M}_c \gg -\dot{M}_2$  this reduces to the same form. As  $\dot{M}_c$  decreases it will approach the limit of  $\dot{M}_c = -\dot{M}_2$ , at which point  $\ddot{M}_c = 0$ . The exact form of the decay will depend on the unreliably known form of  $\mu_c(R)$ , and during the late linear decline viscous heating near  $R_h$  becomes non-negligible. We do not predict the form of the late decay other than to note that if there is some radius  $R_{\text{lim}}$  satisfying

$$\mu(R_{\text{lim}}) \eta c^2 = \frac{R_{\text{lim}}^2}{\Phi}, \quad (18)$$

then the l.h.s. of (18) will give the asymptotic limit of the decay and the accretion luminosity at the beginning of quiescence.

As a final point on the linear decay we note that the viscous instability may cause a range of annuli within the cold disc to enter the hot state and rapidly transfer mass inward. Some of this may enter the inner hot disc, or else may increase the surface density of the subsequent cold disc such that the inner hot disc receives more material at its outer edge. Consequently, small rebrightenings or other artefacts potentially complicate the linear decay.

### 2.3 Continuous derivative

To examine the observed X-ray light curves of transient LMXBs it is useful to examine the constraints on the transition. The gradient of the exponential decay at time  $t_t$  is

$$\dot{L}_X = -\frac{3\nu_{\text{KR}}}{R_{\text{disc}}^2} (L_t - \eta(-\dot{M}_2)c^2), \quad (19)$$

whilst the gradient of the linear decline is given by (16),

$$\dot{L}_X = -\frac{3\nu_{\text{KR}}}{\Phi}. \quad (20)$$

From (3) we adopt

$$R_{\text{disc}}^2 = \Phi L_t, \quad (21)$$

where it is assumed that at the outer disc edge  $H \simeq 0.2R_{\text{disc}}$ . We therefore obtain

$$\dot{L}_X(t_t) = -\frac{3\nu_{\text{KR}}}{\Phi} \left( 1 - \frac{\eta(-\dot{M}_2)c^2}{L_t} \right). \quad (22)$$

In the case that  $-\eta\dot{M}_2c^2$  is small relative to  $L_X$  the gradient of the exponential decay at time  $t_t$  is equal to that of the subsequent linear decline; the first derivative of the X-ray light curve is expected to vary smoothly throughout the decay. If however  $-\eta\dot{M}_2c^2$  cannot be neglected then the linear decline is steeper than the exponential decay at  $t_t$  and a discontinuity in gradient is expected. Whether this is detectable depends on the value of  $-\dot{M}_2$  and the quality of the X-ray data.

Some X-ray light curves, including most of those discussed in this paper, include a knee feature in the decay from outburst. Where this can be explained by an exponential to linear transition with non-negligible  $-\eta\dot{M}_2c^2$  we label it as a ‘brink’. In general the decay light curve may contain multiple knees due to different effects, but we do not expect more than one brink unless the source rebrightens between them such that each occurs at approximately the same luminosity, corresponding to a disc not varying greatly in radius.

## 3 APPLICATION TO OBSERVED X-RAY TRANSIENTS

X-ray light curves from the All-Sky Monitor (ASM) and Proportional Counter Array (PCA) of the *RXTE* space telescope were examined to find examples of decay light curves which fit the template predicted above. We use our analysis to determine distances and accretion disc radii. System parameters from the literature for the objects analysed are collected in Table 1 for comparison with quantities we derive. Since we will be calculating the radius of the accretion disc we calculate from the system parameters the orbital separation  $a$ .

The count rates  $N$  as a function of time  $t$  were fitted with

$$N = (N_t - N_e) \exp\left(-\frac{t - t_t}{\tau_e}\right) + N_e \quad (23)$$

for the exponential phase, where  $N_e$  is the limit of the exponential decay,  $N_t$  is the count rate at the brink, and  $\tau_e$  is the time-scale of the decay. The linear decline is given by

$$N = N_t \left( 1 - \frac{t - t_t}{\tau_l} \right), \quad (24)$$

where  $\tau_l$  is the time after the brink at which the count rate would become zero if the linear decline continued. Using the assumed distance to each source with a hydrogen column density of  $10^{22} \text{ cm}^{-2}$  it is possible to convert the count rates  $N_t$  and  $N_e$  into absolute X-ray luminosities  $L_t$  and  $L_e$ , the X-ray luminosity at the brink and the limit of the exponential decay (corresponding to  $-\dot{M}_2$ ) respectively. For the two systems for which we have simultaneous ASM and PCA light curves, XTE J0929-314 and GRO J1744-28, the ratio of count rates is approximately 31. We assume this conversion to be valid for all sources for comparison purposes, and present luminosities in the 1.5–12 keV range corresponding to the ASM spectral range using an assumed power law spectrum with photon index of  $\Gamma = 2$ . The luminosities thus determined are given in Table 2. We note that if the spectrum differs between systems our deduced  $L_t$  is invalid, though our deduced exponential timescale will be unaffected.

Using (3) and (9) it is possible to calculate the disc radius independently from the measured values of  $N_t$  and  $\tau_e$ ; the result based on  $\tau_e$  is of particular importance as it does not depend on the conversion of count rate to flux but only on a directly observable timescale. It is also possible to determine  $-\dot{M}_2$  from  $N_e$ . Results are given in Table 3; for comparison we have also listed the circularization radius,  $R_{\text{circ}}$ , and the distance between the compact object and the inner Lagrange point,  $b_1$ , for each source based on the values in Table 1. Discussion of the choice of values for  $\Phi$  and  $\nu_{\text{KR}}$  is given in section 4.

### 3.1 4U 1543-475

Fig. 1 shows that the exponential-then-linear fit to the decay from the 2002 outburst of 4U 1543-475 is significantly better than the least-squares regression line. Because no discontinuity is seen in the gradient, the fitting routine used was based on the continuous derivative model (see section 2.3). Previous outbursts were reported in 1971, 1983 and 1992. The source therefore spends only a small fraction of its time in outburst, suggesting that  $-\dot{M}_2$  is small compared with the central accretion rate during outburst, consistent with the source’s failure to display a broken gradient.

### 3.2 SAX J 1808.4-3658

SAX J 1808.4-3658 was first detected in outburst in 1996 and has subsequently shown outbursts in 1998, 2000, 2002, and 2005. Hence it is expected that the ratio of  $-\dot{M}_2$  to the peak central accretion rate is much higher than in 4U 1543-475. This is consistent with the appearance of a broken decay in the two well observed outbursts, shown in Figs. 2 and 3. Each light curve is well fitted by a decay that is exponential towards a positive limit followed by a sharp gradient discontinuity (brink) leading to a linear decline. The fit to the 1998 outburst includes all points that can be confirmed to occur during the decay; the observation at day 16 of Fig. 2 may belong to a period of constant luminosity or even an unsteady rise to outburst, while the observations around day 33 of Fig. 2 may involve a rebrightening. Even if this is not the case the late linear decline is expected to become increasingly complex, as we noted in Section 2.2. Comparison with Fig. 3 shows that the brink occurs at approximately

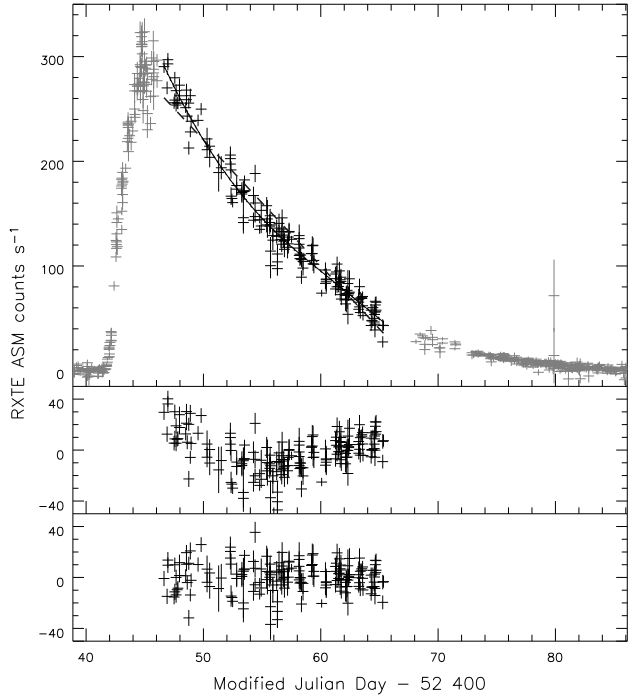


**Figure 1.** **Top panel:** The fitted ASM light curve of 4U 1543-475. The solid line shows the exponential-then-linear fit, the dashed line indicates the best linear fit. The data shown in grey were not included in the fit, lying before and after the period of interest. **Middle panel:** Residuals to the linear fit. **Bottom panel:** Residuals to the exponential/linear fit.

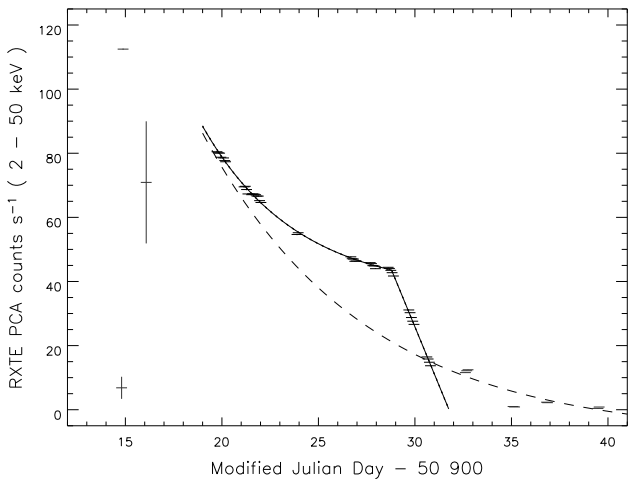


**Figure 2.** The fitted PCA light curve of the 1998 outburst of XTE J 1808.4-3658. The dashed line indicates the fit of SCK.

the same count rate in both cases. This is expected if  $R_{\text{disc}}$  remains constant (i.e.  $L_t$  is the same).

The dashed line in Fig. 2 indicates the fit proposed by SCK, in which they identified the surplus around the brink as a secondary maximum. We disagree and view their fit as inadequate in having a negative limit to the exponential decay. It is possible that features in other decay light curves identified as secondary maxima but having monotonically decreasing X-ray flux have the same explanation.

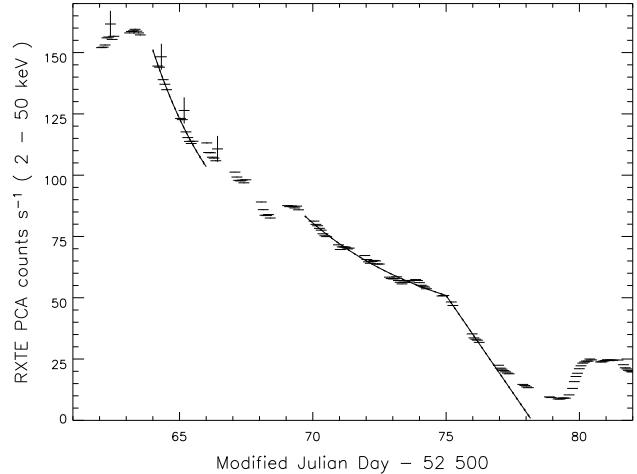


**Figure 3.** The fitted PCA light curve of the 2002 outburst of XTE J 1808.4-3658

A second issue in Fig. 3 is the broken nature of the light curve prior to the brink. Whilst we do not have a detailed explanation for this, we speculate that it may be associated with some regions of the disc being self-shadowed and initially remaining in the cool state. 3D hydrodynamic simulations (e.g. Foulkes, Haswell & Murray 2006) show self-shadowing is likely, due to spiral density waves and irradiated disc warping (c.f. Pringle 1986). Consequently the effective area of the hot disc, the quantity probably corresponding to our measurement of  $R_{\text{disc}}^2$ , increases during the decay in an apparently stepwise manner, introducing new material into the hot disc and therefore resetting the central luminosity to a higher value. This view is supported by the fact that fitting the region around day 65 of Fig. 3 indicates a shorter exponential time-scale than from day 70 to the brink, corresponding to a smaller outer radius of the hot region. By day 70 we assume that the entire disc is in the hot state. The growing irradiated area could lead to an actual increase in  $L_X$ , hence it is an explanation for a type of secondary maximum. It is possible that the light curve will monotonically decline despite the growing irradiated area, hence producing knees in the light curve. The light curve of SAX J 1808.4-3658 around day 67 of Fig. 3 is suggestive of this behaviour.

### 3.3 XTE J 1751-305

XTE J 1751-305 was first detected during its 2002 outburst, shown in Fig. 4, and a second outburst was observed in 2005. If this repetition interval is normal for the system, it indicates a ratio of  $-\dot{M}_2$  to peak central accretion rate more similar to that of SAX J 1808.4-3658 than to 4U 1543-475. Consistent with this, the 2002 decay light curve has a shape similar to those of SAX J 1808.4-3658 in that a smooth exponential decay is broken by occasional rebrightenings. Therefore only the last portion, appearing to correspond to a single smooth decay, is fitted. The linear portion of this decay terminates at a constant level. In accordance with (17) we interpret this as the rate at which mass can be transferred through the mostly cold disc; this rate will continue during quiescence whilst the disc mass increases.

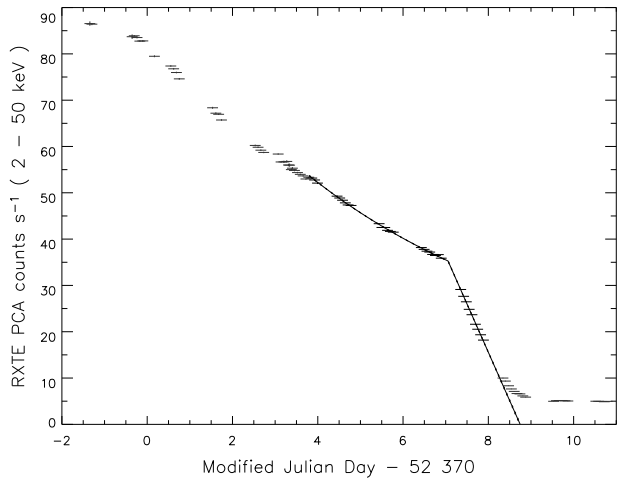


**Figure 4.** The PCA light curve of the 2002 April outburst of XTE J 1751-305, fitted after MJD 52 373.

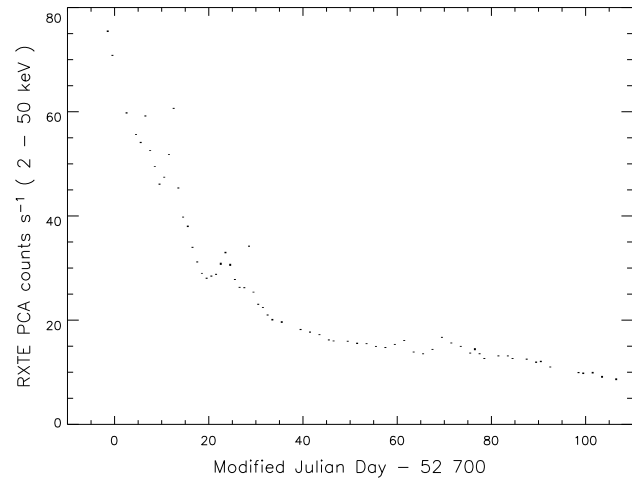


**Figure 6.** The PCA light curve of XTE J 1807-294

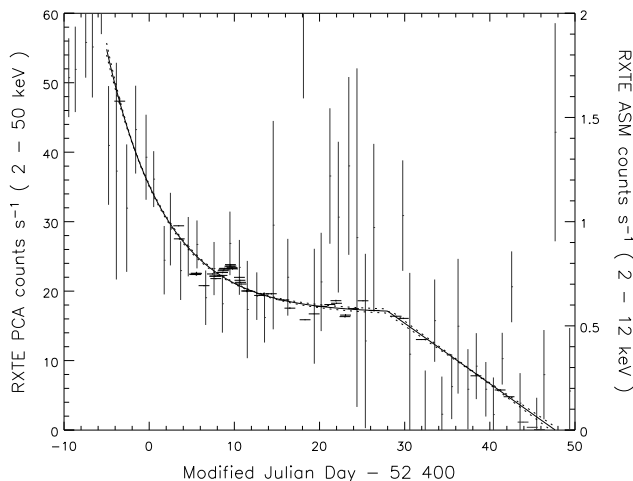


**Figure 5.** The fitted PCA light curve of XTE J 0929-314. The ASM light curve, suitably scaled, is overplotted in grey.

### 3.4 XTE J 0929-314

A third observed example of the brink is found in the only observed (2002) outburst of XTE J 0929-314. Here the overall shape before the brink is exponential, but a maximum at about day 10 of Fig. 5 and a minimum at about day 19 are anomalous. Possibly the outer edge of the disc remained cold until late in the exponential decay and several secondary maxima of the type already discussed have occurred.

### 3.5 XTE J 1807-294

XTE J 1807-294 is, like SAX J 1808.4-3658, XTE J 1751-305 and XTE J 0929-314, one of seven known milli-second pulsar (MSP) systems. MSPs have short orbital periods and hence small and therefore relatively simple discs. We therefore expect the X-ray light curve of XTE J 1807-294 to also display the brinked decay seen in the first three. Fig. 6 does not appear to lend itself to this type of fitting, and we have been unable to obtain reasonable fitting parameters. One possible

explanation is that the linear decay had already begun at the start of the observed light curve; in this case the brink count rate must be around fifty per cent greater than that seen in SAX J 1808.4-3658. The orbital separation of XTE J 1807-294 (c.f. Table 1) is half that of SAX J 1808.4-3658, so the disc must be correspondingly smaller. A high value of  $N_t$  can only be accounted for if XTE J 1807-294 is at a distance of less than about 1 kpc so the luminosity remains low while the countrate is high. Conversely, if the light curve corresponds to the exponential portion with several rebrightenings, the maximum value of  $N_t$  may be 15, with the light curve after day 80 tentatively assumed to be linear. If the disc is half the radius of that of SAX J 1808.4-3658, in proportion to the orbital separation, (12) indicates that the brink luminosity will be one quarter that of SAX J 1808.4-3658. The PCA count rate at the proposed brink is one quarter that of SAX J 1808.4-3658, indicating a similar source distance of  $D \simeq 2$  kpc. We deem the latter explanation more likely, and suspect that the exponential decay of XTE J 1807-294 is complicated by self-shadowing of the disc.

The more extreme mass ratio of XTE J 1807-294 than SAX J 1808.4-3658, indicated in Table 1, suggests that the accretion disc radius in XTE J 1807-294 is a larger fraction of the orbital separation, indicating a larger brink luminosity than assumed above, increasing the distance estimates in both cases. A lower value of  $N_t$  is possible in the second case, which would also indicate a greater source distance.

### 3.6 GRO J 1744-28

The earliest part of the *RXTE* light curve of GRO J 1744-28, shown in Fig. 7, shows the system already in outburst; the first PCA data are consistent with the outburst decay. The light curve has a brink just after day 170 in Fig. 7. GRO J 1744-28 entered a relatively quiescent period in 1996 April ( $\sim$ day 200 of Fig. 7), punctuated by a mini-outburst shown inset in Fig. 7 following day 260 which reached less than half the brink luminosity. A second outburst, smaller than the 1996 outburst, followed during the first four months of 1997. Since then the system has been quiescent. Fig. 8 shows the decay from the 1997 outburst, in which a brink is clearly present. Our confidence in the identification of these

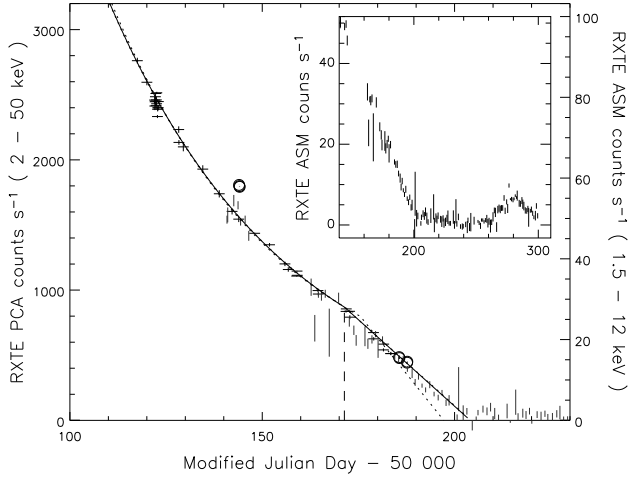


**Figure 7.** GRO J1744-28 light curve for the decay of 1996. Points shown in black are the PCA data; circles indicate those data not fitted. ASM data is shown in grey to mark the behaviour during a gap in the PCA coverage. The solid line indicates the best-fitting decay model; the dotted lines indicate the error bars on the model. The dashed line marks the best-fitting date of the brink. Inset: The ASM light curve for the late decay and subsequent mini-outburst.

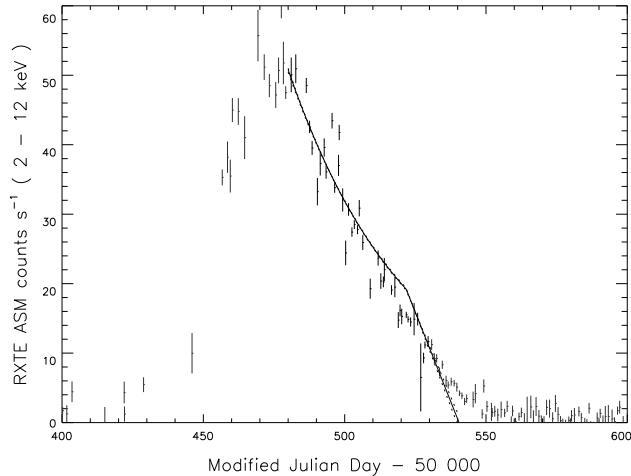


**Figure 8.** GRO J1744-28 light curve for the decay of 1997. Solid and dotted lines mark the best fit and uncertainty, as in Fig. 7.

two knees as brinks is increased by their similarity in luminosity.

### 3.7 GX 339-4

As shown in Fig. 9, GX 339-4 follows an exponential decay to less than 10 per cent of its outburst maximum, a much smaller fraction than is exhibited by the other systems considered so far. The relatively few existing points fit the brinked decay model well. The late decay departs smoothly from the linear decline, in line with expectations (c.f. section 2.2 eqn. 15 and following comments).

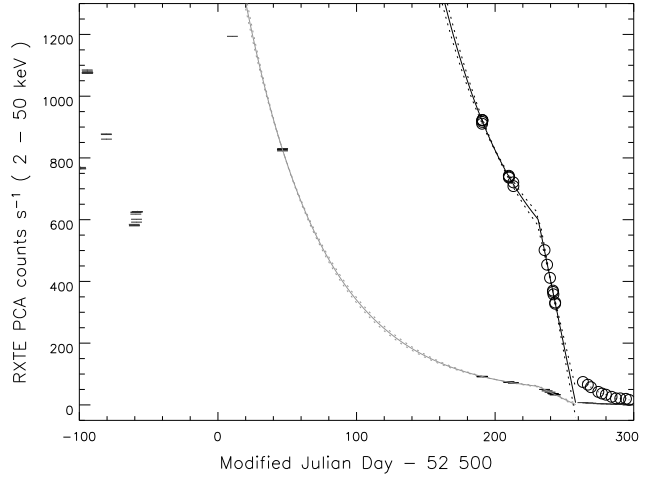


**Figure 9.** The fitted PCA light curve of GX 339-4. Circles mark data points where the y-scale has been stretched by a factor of ten.

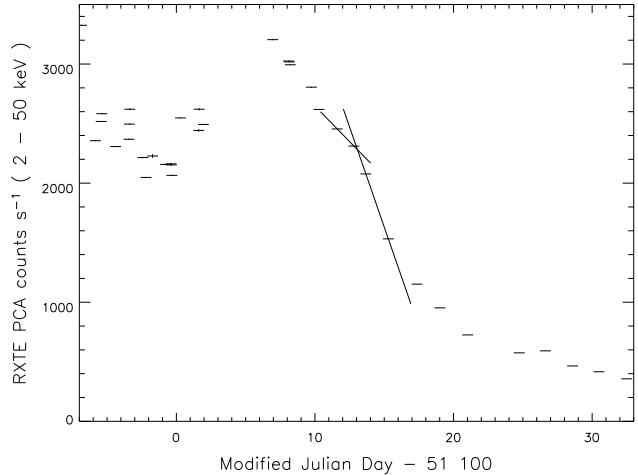


**Figure 10.** The PCA light curve of XTE J1550-564. Not enough data cover the decay to be able to perform useful fitting, but the presence of a knee in the decay is indicated by the four points through which lines have been drawn.

### 3.8 XTE J1550-564

Although not enough data exist to be able to establish the parameters of the brinked decay, a knee occurs in the PCA light curve, which has been marked in Fig. 10. Interpreting this as the brink it is therefore possible to calculate  $R_{\text{disc}}$  based on  $N_t$  but no other system parameters.

### 3.9 GRO J1655-40

The ASM light curve of GRO J1655-40 shows one outburst, starting in 1996 April and persisting until 1997 August. This outburst is broadly divided into two broad peaks, of which the decay of the second is shown. Although the system had been in outburst for a considerable time, Hynes et al. (1998) note that no stable hot disc state exists for luminosities less than the Eddington luminosity; it is therefore unclear whether material from the outer disc edge participated in

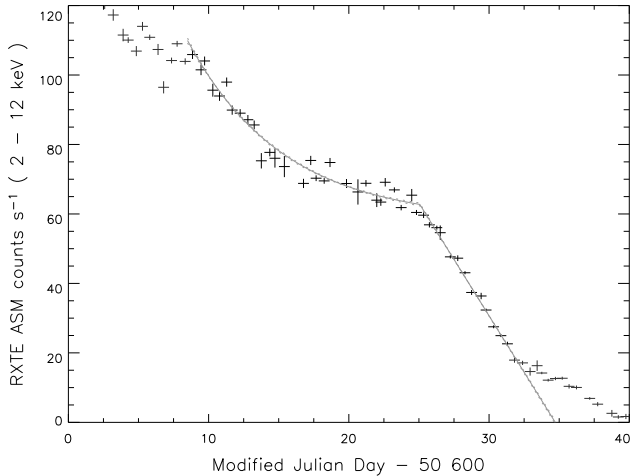


**Figure 11.** The ASM light curve of GRO J 1655-40. Although the calculated error on the brink luminosity is less than 1 ASM count  $s^{-1}$ , we note by examination that the brink in the light curve may be uncertain by 5 ASM counts  $s^{-1}$  if some of the scatter is intrinsic variability.

the outburst. As shown in Table 3, the accretion disc radius calculated from the brink luminosity and the exponential timescale match each other, but are considerably less than the system’s circularization radius. This may indicate that the mechanism examined here is applicable, but acts on a small inner disc region rather than on the disc as a whole. Possibly this second peak is caused by a high surface density remnant left by the preceding outburst activity.

GRO J 1655-40 returned to outburst in 2005; if the average flux between the beginning of the two successive outbursts is taken as an indicator of  $-\dot{M}_2$ , this value is found to lie below the brink by a factor of three. The mass transfer rate from the secondary star may be enhanced during outburst, but it is likely that the mass flow onto the (constant radius) outer edge of the hot disc during the exponential phase is supplied from additional disc structures rather than from the secondary directly. The complexity of the disc in this system does not necessarily invalidate the application of this model during at least some phases of the decay.

### 3.10 4U 1705-44

No PCA light curves for 4U 1705-44 are available, so the best evidence for our model being applicable to this system comes from the ASM light curve. This shows numerous outbursts, the decays of which are shown in Fig. 12. A range of smaller outbursts also occur which are not shown in Fig. 12. Arrows mark features in the light curve that we have interpreted as the brink of each decay; using these as part of the initial conditions for finding a best fit we obtained the best-fitting decays overplotted. Clearly there is substantial variation in the height of the brink, which indicates variation in the radius of the disc. In order to explain this we used the ASM light curve to assess the fluence of each outburst. A greater fluence suggests a greater initial disc mass, which leads us to expect positive correlation between the fluence and calculated disc radius. Relative fluences are given in Table 3,

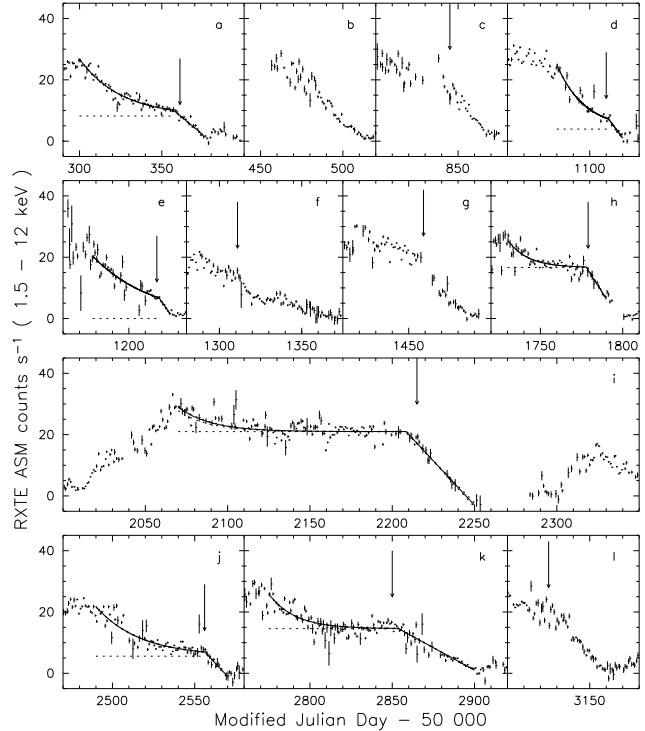


**Figure 12.** The ASM light curve for all decays from major outburst seen in 4U 1705-44 by the instrument to date. Arrows marks points in the light curve where a knee between an exponential decay and a linear one may be present, assigned by eye and used as initial conditions for the fitting. Horizontal dotted lines indicate the limit of the exponential decay. Each outburst has been assigned a letter for reference.

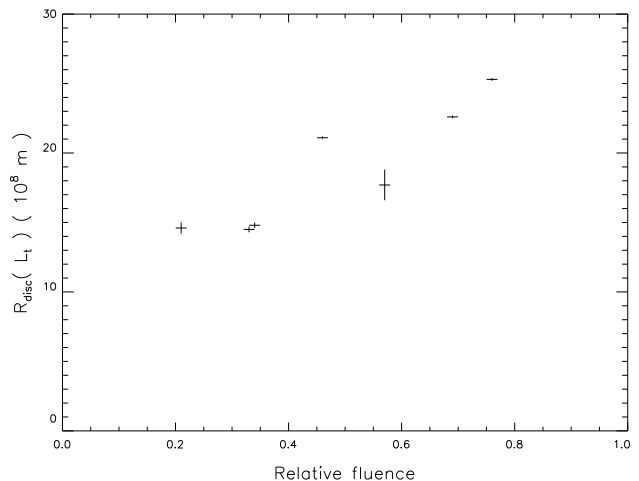


**Figure 13.** Disc radius versus outburst fluence for the seven fitted outbursts of 4U 1705-44.

and Fig. 13 shows a positive correlation between outburst fluence and  $R_{\text{disc}}(L_t)$ .

If at least some of the knees marked in Fig. 12 actually correspond to the disc radius mechanism being considered (i.e. they are brinks), then substantial variation in the radius is seen. Furthermore, the limit of the exponential decay is clearly in several cases below the mean long term count rate

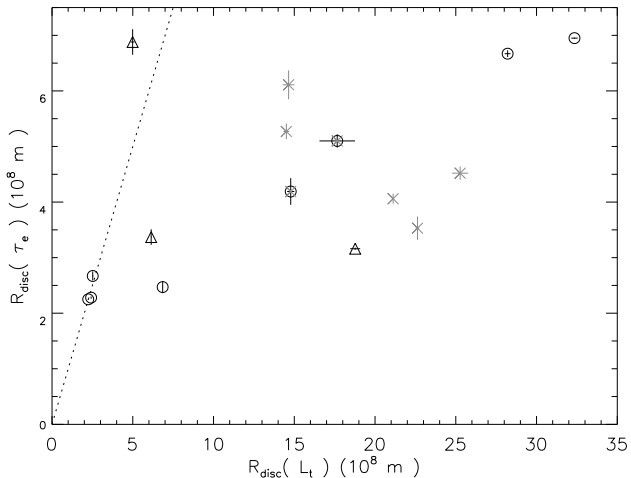


**Figure 14.** The relation between the radius as determined from the brink luminosity against that based on the exponential timescale. Circles mark neutron star systems, and triangles black holes; individual points can be identified using Table 3. Crosses mark decays of 4U 1705-44 other than *a* and *d*, as described in the text. A diagonal, dotted line marks  $R_{\text{disc}}(L_t) = R_{\text{disc}}(\tau_e)$ .

of 12 counts per second, based on the numerical integration of the ASM light curve. We account for this by the additional theory given in section 5.

#### 4 SOURCE DATA AND BEST-FITTING PARAMETERS

To force the disc radii based on  $\tau_e$  to lie within the range  $R_{\text{circ}} < R_{\text{disc}}(\tau_e) < b$  for the two best described systems, SAX J1808.4-3658 and XTE J0929-314, the viscosity of  $\nu_{\text{KR}} = 4 \times 10^{10} \text{ m}^2 \text{ s}^{-1}$  was adopted, close to the value of  $10^{11} \text{ m}^2 \text{ s}^{-1}$  proposed by KR. To make  $R_{\text{disc}}(L_t)$  consistent with  $R_{\text{disc}}(\tau_e)$  for most of the neutron star systems a value of  $\Phi = 1.3 \times 10^{-12} \text{ m}^2 \text{ s J}^{-1}$  was adopted. A better fit was found for the black hole systems by reducing  $\Phi$  by a factor of ten, consistent with the extra factor of  $H_0$  discussed in the introduction.  $\Phi$  is somewhat small compared with the range of  $4 < \Phi / (10^{-12} \text{ m}^2 \text{ s J}^{-1}) < 9$  adopted by KR. Furthermore, since  $R_{\text{disc}}$  is based on  $\Phi L_t$ , our systematic underestimate of  $L_t$  by considering only the flux in the 1.5–12 keV band suggests a yet smaller value of  $\Phi$ . Calculated disc radii using these parameter values are given in Table 3.

Fig. 14 shows the relation between the values of  $R_{\text{disc}}$  calculated from  $L_t$  and  $\tau_e$ . We note that for 4U 1705-44 the results would be more consistent if we adopted the lower value of  $\Phi$ , appropriate to black hole systems. This may reflect differences in the source spectrum as well as intrinsic differences in  $\Phi$  since we have assumed the same relation between 1.5–12 keV count rate and total X-ray flux for all systems. In addition to this effect, we note that the results for 4U 1705-44 in Fig. 14 do not lie on a straight line.

To examine this issue we first determined a best-fitting value of  $\Phi/\nu_{\text{KR}}$  from decays *a* and *d*, which we deem the strongest results by inspection of the light curve. We then demanded that this value of  $\Phi/\nu_{\text{KR}}$  apply to each decay of 4U 1705-44. In Fig. 15 we show the effect this has on the fits, plotting the residuals for the individual best-fits, and for the

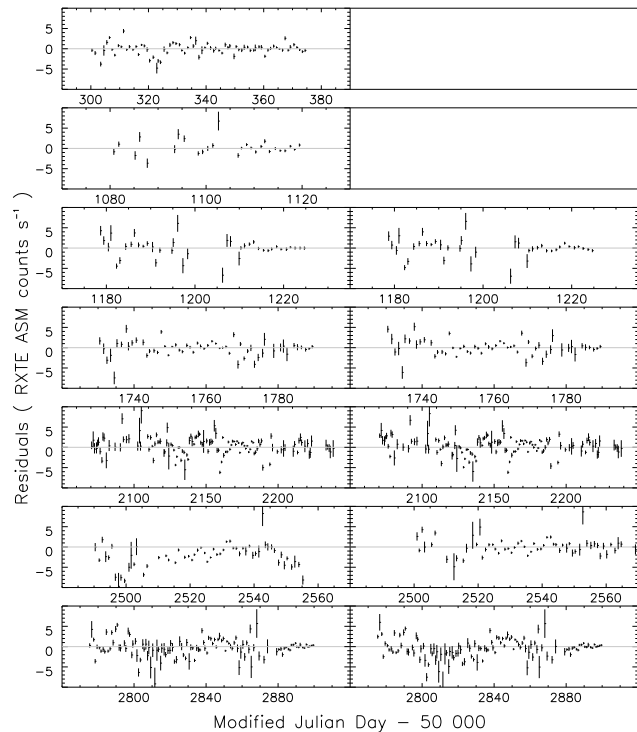


**Figure 15.** Residuals to the fitted portions of the *RXTE* ASM light curve of 4U 1705-44. **Left column:** using best-fitting parameters for each individual decay. **Right column:** Relating the brink luminosity to  $\tau_e$  by  $N_t/\tau_e = 2.8 \times 10^{-5} \text{ ASM counts s}^{-2}$  in all cases.

constrained fits. If the original fits were strongly determined by the data, we would expect the residuals to appear significantly worse in the constrained fits. In contrast, we find that in some cases the residuals appear to improve, and in none is the fit substantially worse; the reduced  $\chi^2$  for the whole set of fits increases from 11.4 when  $L_t$  and  $\tau_e$  are optimized individually to 12.1 for the constrained fitting. We note that technique is only applicable when comparing decays of the same source, where variation in the quantity  $\Phi/\nu_{\text{KR}}$  is minimized.

The large value of  $R_{\text{disc}}(L_t)$  for XTE J1751-305 may be again the result of spectral differences, or in this case may be the result of an erroneous source distance estimate. XTE J1751-305 has been assumed to lie at a distance of 8 kpc, being possibly associated with the Galactic Centre (e.g. Gierliński & Poutanen 2005); if the true distance is more like 3 kpc then the two values of  $R_{\text{disc}}$  will be approximately equal.

The increasing value of  $R_{\text{disc}}(\tau_e)$  for the 2002 decay of SAX J1808.4-3658 and the erratically increasing luminosity between days 65 and 70 of Fig. 3 are both consistent with the interpretation that the outer disc edge was not in the hot state at the beginning of the decay. As such, the disc radius measured corresponds at first to a hot disc smaller than the disc as a whole, which is therefore depleted on a shorter timescale. At some point the outer disc is heated and enters the hot state. As well as increasing the timescale of the decay, this introduces extra material into the hot disc, causing rebrightening.



Source	$P_{\text{orbit}}$ [min]	$P_{\text{spin}}$ [ms]	$a$ [ $10^8$ m]	$M_2$ [ $M_{\odot}$ ]	Distance [kpc]	
XTE J 0929-314	43.6 <sup>a</sup>	5.4 <sup>a</sup>	3.2	0.008–0.03 <sup>a</sup>	5 <sup>a</sup>	NS
4U 1543-475	1617 ± 12 <sup>b</sup>	–	73 ± 4 <sup>c</sup>	2.7 ± 1.0 <sup>c</sup>	7.5 ± 1.0 <sup>c</sup>	BH
XTE J 1550-564	2235 ± 14 <sup>d</sup>	–	86–92 <sup>d</sup>	1.4 ± 0.5 <sup>d</sup>	2.8–7.6 <sup>d</sup>	BH
GRO J 1655-40	3775.1 ± 0.2 <sup>e</sup>	–	117 ± 1 <sup>e</sup>	2.34 ± 0.12 <sup>e</sup>	3.2 <sup>e</sup>	BH
4U 1705-44	–	–	–	–	7.3 ± 1.0 <sup>f</sup>	NS
GRO J 1744-28	17000 <sup>g</sup>	–	190 <sup>g</sup>	0.2–0.7 <sup>g</sup>	8.5 <sup>h</sup>	NS
XTE J 1751-305	42 <sup>i</sup>	2.3 <sup>i</sup>	3.1	0.013–0.035 <sup>i</sup>	–	NS
XTE J 1807-294	40 <sup>j</sup>	5.25 <sup>j</sup>	3.0	0.01–0.022 <sup>k</sup>	–	NS
SAX J 1808.4-3658	120.8 <sup>l</sup>	2.5 <sup>l</sup>	6.3	0.04–0.1 <sup>l</sup>	2.5 <sup>m</sup>	NS
GX 339-4	2500 <sup>n</sup>	–	80–120 <sup>n</sup>	≲ 1.1 <sup>n</sup>	15 <sup>n</sup>	BH

a: Galloway et al. (2002)    f: Haberl & Titarchuk (1995)    k: Falanga et al. (2005)  
 b: Orosz et al. (1998)    g: Rappaport & Joss (1997)    l: Chakrabarty & Morgan (1998)  
 c: Park et al. (2004)    h: Nishiuchi et al. (1999)    m: in 't Zand et al. (2001)  
 d: Orosz et al. (2002)    i: Markwardt et al. (2002)    n: Hynes et al. (2004)  
 e: Orosz & Bailyn (1997)    j: Campana et al. (2003)

**Table 1.** System parameters from the literature. Orbital separation  $a$  is based on a  $1.4M_{\odot}$  neutron star where an accretor mass is not available.

Decay	$L_t$ [ $10^{27}$ J s <sup>-1</sup> ]	$L_e$ [ $10^{27}$ J s <sup>-1</sup> ]	$\tau_e$ [days]	$\tau_l$ [days]
XTE J 0929-314	49 ± 1	48 ± 1	6.9 ± 0.4	19.7 ± 1.2
4U 1543-475	27100 ± 900		12.05 ± 0.13	
XTE J 1550-564	11200 ± 100			
GRO J 1655-40	2900 ± 20	2610 ± 50	13.7 ± 0.9	19.3 ± 0.3
4U 1705-44 a	2400 ± 300	1920 ± 80	25.1 ± 1.2	22.7 ± 1.4
4U 1705-44 d	1680 ± 50	900 ± 200	16.9 ± 1.9	10.0 ± 0.6
4U 1705-44 e	1650 ± 80	0–220	36 ± 3	8.4 ± 0.8
4U 1705-44 h	3940 ± 40	3900 ± 50	12.0 ± 1.4	19.8 ± 1.7
4U 1705-44 i	4910 ± 20	4910 ± 20	19.7 ± 1.0	36.4 ± 1.6
4U 1705-44 j	1620 ± 40	4170 ± 30	26.8 ± 1.4	12.0 ± 1.7
4U 1705-44 k	3430 ± 20	3410 ± 20	15.9 ± 0.7	50.0 ± 0.9
GRO J 1744-28 1996	8050 ± 100	0–40	46.61 ± 0.12	21.4 ± 1.0
GRO J 1744-28 1997	6120 ± 80	0–170	42.9 ± 0.8	18.7 ± 1.2
XTE J 1751-305	361 ± 1	110 ± 30	5.9 ± 0.5	1.69 ± 0.02
SAX J 1808.4-3658 1998	38.54 ± 0.03	32.3 ± 0.2	4.89 ± 0.06	2.978 ± 0.007
SAX J 1808.4-3658 2002a		50 ± 7	2.8 ± 0.3	
SAX J 1808.4-3658 2002b	45.1 ± 0.1	29.6 ± 0.6	5.0 ± 0.1	3.22 ± 0.03
GX 339-4	1916 ± 90	900 ± 200	57 ± 3	27 ± 4

**Table 2.** Decay light curve parameters. Luminosities are based on the photon index and distance from Table 1 and values of  $N_H$  from the same sources, and are stated for a spectral range of 1.5–12 keV. For consistency with Figs. 7 and 5 we take 1 ASM count s<sup>-1</sup> to equal 31 PCA counts s<sup>-1</sup> for our purposes, suggesting that  $\Gamma \simeq 2.1$ .

## 5 MODIFIED EXPONENTIAL LIMIT

We have assumed in the initial model that the limit of the exponential decay is equal to the assumed constant mass transfer rate from the donor star. This requires that the hot disc is capable of supporting the additional mass flux  $-\dot{M}_2$  at all times and radii. However, the exponential nature of the decay itself implies that as the hot disc is depleted in surface density, its mass transfer rate falls. The mass transfer equation of the hot disc is linear in surface density, which can therefore be decomposed into two components; one representing the decay analogous to an unfed disc, the other corresponding to the effects of feeding the hot disc at the rate  $-\dot{M}_2$ . The former component we denote  $\Sigma_e$  and the latter  $\Sigma_2$ . Because the viscosity of the accretion disc depends on temperature, and the temperature is declining during the decay, it is necessary for  $\Sigma_2$  to increase with time if it is to

sustain the same mass flux, implying that the corresponding flux  $\mu_2$  must decrease inwards. Thus the limit of the central mass accretion rate does not correspond to  $-\dot{M}_2$ , but rather  $\mu_2(R_{\text{in}})$ . The relevance of this issue is made clear by the light curves of 4U 1705-44, in which the limit of the exponential decay is often below the long term mean count rate of 12 ASM counts s<sup>-1</sup>.

The standard derivation of the diffusion equation (e.g. Pringle 1981) can be used to give the mass transfer rate inward through the disc  $\mu$  as

$$\mu = 6\pi R^{1/2} (\nu \Sigma R^{1/2})'. \quad (25)$$

Using the relation

$$\mu' = 2\pi R \dot{\Sigma}, \quad (26)$$

we derive equation 9 of King (1998) as expected. We require

Decay	$R_{\text{circ}}$ [ $10^8$ m ]	$b_1$ [ $10^8$ m ]	$R_{\text{disc}}(L_t)$ [ $10^8$ m ]	$R_{\text{disc}}(\tau_e)$ [ $10^8$ m ]	Relative fluence	$-\dot{M}_2$ [ $10^{-12} M_{\odot} \text{ yr}^{-1}$ ]
XTE J 0929-314	1.5–1.9	2.63–2.82	$2.52 \pm 0.03$	$2.67 \pm 0.08$		$84 \pm 2$
4U 1543-475	12.7–17.1	43.4–48.7	$18.8 \pm 0.3$	$3.16 \pm 0.02$		–
XTE J 1550-564	20.0–26.4	58.5–64.2	$12.15 \pm 0.05$	–		–
GRO J 1655-40	21.3–22.1	70.9–72.1	$6.14 \pm 0.02$	$3.43 \pm 0.11$		$4600 \pm 100$
4U 1705-44 a	–	–	$17.7 \pm 1.1$	$5.10 \pm 0.12$	0.57	$3400 \pm 200$
4U 1705-44 b	–	–	–	–	0.32	–
4U 1705-44 c	–	–	–	–	1.00	–
4U 1705-44 d	–	–	$14.8 \pm 0.2$	$4.2 \pm 0.2$	0.34	$1600 \pm 400$
4U 1705-44 e	–	–	$14.6 \pm 0.4$	$6.1 \pm 0.3$	0.21	$\lesssim 400$
4U 1705-44 f	–	–	–	–	0.21	–
4U 1705-44 g	–	–	–	–	0.30	–
4U 1705-44 h	–	–	$22.6 \pm 0.12$	$3.5 \pm 0.2$	0.69	$6900 \pm 200$
4U 1705-44 i	–	–	$25.3 \pm 0.05$	$4.52 \pm 0.12$	0.76	$8600 \pm 50$
4U 1705-44 j	–	–	$14.5 \pm 0.18$	$5.27 \pm 0.14$	0.33	$7300 \pm 50$
4U 1705-44 k	–	–	$21.1 \pm 0.06$	$4.06 \pm 0.09$	0.46	$6000 \pm 50$
4U 1705-44 l	–	–	–	–	0.29	–
GRO J 1744-28 1996	32.5–52.3	112.1–133.9	$32.3 \pm 0.2$	$6.95 \pm 0.01$		$\lesssim 70$
GRO J 1744-28 1997	32.5–52.3	112.1–133.9	$28.2 \pm 0.2$	$6.67 \pm 0.06$		$\lesssim 300$
XTE J 1751-305	1.4–1.7	2.5–2.7	$6.85 \pm 0.01$	$2.47 \pm 0.11$		$200 \pm 50$
SAX J 1808.4-3658 1998	2.06–2.71	4.68–5.07	$2.238 \pm 0.001$	$2.252 \pm 0.014$		$57 \pm 4$
SAX J 1808.4-3658 2002a	2.06–2.71	4.68–5.07	–	$1.70 \pm 0.09$		$90 \pm 10$
SAX J 1808.4-3658 2002b	2.06–2.71	4.68–5.07	$2.421 \pm 0.003$	$2.28 \pm 0.02$		$51.8 \pm 1.1$
GX 339-4	$> 23$	$> 66$	$4.99 \pm 0.12$	$6.88 \pm 0.23$		$1600 \pm 400$

**Table 3.** System radii and mass transfer rate. The two values of  $R_{\text{disc}}$  and  $-\dot{M}_2$  are calculated from the X-ray light curves;  $R_{\text{circ}}$  and  $b_1$  are calculated from the data in Table 1. Errors exclude the effect of the uncertainty in source distance.

the form given in (25) to prevent a constant of integration arising.

To make use of (25) we must adopt an appropriate form for the viscosity  $\nu$ . We use the  $\alpha$ -viscosity form

$$\nu = \alpha c_s H, \quad (27)$$

where  $c_s$  is the sound speed, and the scale height is given by equation 2 of King (1998);

$$H = c_s \left( \frac{R^3}{GM_1} \right)^{1/2}. \quad (28)$$

Using (1) to substitute for  $T$  and assuming that  $H(R)$  is a power law we obtain

$$H = \left( \frac{k}{GM_1 m} \right)^{4/7} \left( \frac{(1-A)(n-1)}{4\pi\sigma} \right)^{1/7} L_X^{1/7} R^{9/7}, \quad (29)$$

for a mean particle mass  $m \simeq m_p$ . We write (29) in terms of constant  $H_0$  as

$$H = H_0 R_{\text{disc}} \left( \frac{L_X}{L_t} \right)^{1/7} \left( \frac{R}{R_{\text{disc}}} \right)^n, \quad (30)$$

where  $n = 9/7$  is derived and  $H_0 \simeq 0.2$  is adopted from KR. Burderi, King & Szuszkiewicz (1998) note that if the X-ray flux is assumed to be absorbed at the mid-plane, the power law index is changed to  $45/38$ ; we therefore consider values of  $45/38 \leq n \leq 9/7$  as valid to simplify subsequent derivation. Using this form for  $H$  in (1) to derive the viscosity we find that

$$\nu = \nu_0 \left( \frac{L_X}{L_t} \right)^{2/7} \left( \frac{R}{R_{\text{disc}}} \right)^{(9n-3)/8}, \quad (31)$$

where  $\nu_0$  is defined as

$$\nu_0 = \alpha \left( \frac{k^4 L_t (1-A)(n-1)}{4\pi\sigma m^4} \right)^{1/8} H_0^{9/8} R_{\text{disc}}^{3/4}. \quad (32)$$

We simplify (31) by adopting  $n = 11/9$ , so (25) becomes

$$\mu = \frac{6\pi\nu_0}{R_{\text{disc}}} \left( \frac{L_X}{L_t} \right)^{2/7} R^{1/2} (\Sigma R^{3/2})'. \quad (33)$$

If we impose  $\mu = -\dot{M}_2$  for all radii we obtain

$$\Sigma_2 = \frac{-\dot{M}_2}{3\pi\nu_0} \left( \frac{L_X}{L_t} \right)^{-2/7} \frac{R_{\text{disc}}}{R}, \quad (34)$$

corresponding to a total contribution to mass in the hot disc of

$$m_2 = \frac{-2\dot{M}_2}{3\nu_0} \left( \frac{L_X}{L_t} \right)^{-2/7} R_{\text{disc}}^2, \quad (35)$$

where the radius of the inner disc edge is much smaller than  $R_{\text{disc}}$ . As  $L_X$  decreases, a greater surface density and total mass is required to transport the same  $-\dot{M}_2$  inward, so some of this material must be absorbed to increase the surface density. For a typical luminosity at the beginning of the exponential phase 2.5 times greater than  $L_t$  the change in mass required is

$$\frac{\Delta m_2}{\dot{M}_2} = \frac{2R_{\text{disc}}^2}{3\nu_0} (1 - 2.5^{-2/7}). \quad (36)$$

Examining 4U 1705-44, for which we have the largest mean luminosity relative to  $L_t$ , we find a mean long term count rate of  $12 \text{ ASM counts s}^{-1}$ , whereas the limit of the decay  $a$  for instance is  $8.2 \text{ ASM counts s}^{-1}$ . Taken over an exponential phase duration of 57 days this makes the l.h.s. of (36) equivalent to  $1.9 \times 10^7$  ASM units of mass. Using the conversion factor from WebPIMMS of  $1 \text{ ASM count s}^{-1} =$

$4 \times 10^{-13} \text{ J s}^{-1} \text{ m}^{-2}$ , at a distance of 7.3 kpc this integrated flux is equivalent to  $3 \times 10^{20} \text{ kg}$ . Using  $\nu_{\text{KR}} = 4 \times 10^{10} \text{ m}^{-2} \text{ s}^{-1}$  (as in Table 3) we find

$$R_{\text{disc}} \simeq 6.4 \times 10^8 \text{ m}, \quad (37)$$

in strong agreement with the values given in Table 3 despite the weakness of the derivation. In principle it is necessary to simultaneously derive the time and radius dependencies of  $\mu$  given the outer boundary condition of  $\mu(R_{\text{disc}}) = -\dot{M}_2$ , but this is beyond the scope of this paper.

## 6 CONCLUSIONS

A knee in the light curve of the decay from outburst of an transient LMXB is a natural consequence of mass transfer onto the outer edge of the disc, since this supply is effectively cut off from the compact object when the outer disc enters the cool low-viscosity state. When the knee can be interpreted in this way we refer to it as a brink, since knees of other types may be seen in the decay outburst. The X-ray luminosity at which the brink occurs is that at which the outer disc edge is just kept hot by central illumination, allowing this radius to be calculated. In addition, the exponential time-scale of the decay gives a second measure of the disc radius; these two estimates are in good agreement. By examining systems with well constrained disc radii we deduced values of the constants  $\Phi$  and  $\nu_{\text{KR}}$  required to perform the calculations. This allows more accurate results to be obtained in other systems. Where the source distance is poorly constrained, the timescale  $\tau_e$  allows the absolute luminosity  $L_t$  to be estimated, providing a measure of source distance.

As well as ‘secondary maxima’ associated with the brink, we have identified maxima whose natural explanation is the discontinuous increase in the radius of the hot disc during outburst. This increase arises from initially self-shadowed disc regions becoming irradiated. This process can occur until the whole disc is in the hot state. It is characteristic for the time-scale of the exponential decay to increase with each such maximum, and it is expected that the limit of each exponential decay will also increase. Although we do not have sufficient data to examine the matter in detail, it is probable that some secondary ‘maxima’ of this type will also involve monotonic decay, and therefore probably will appear as a knee in the X-ray light curve.

Current instrumentation is capable of measuring the light curves of X-ray transients in M31, for example Trudolyubov, Priedhorsky & Cordova (2006) show part of a 2004 July decay of XMM J004315.5+412440. While this light curve, with only 4 data points over 3 consecutive days, is too sparse to allow us to deduce any parameters from fitting the decay, our method could be applied to better-sampled extragalactic transient decays. Since the distance is relatively well-known for objects in external galaxies, we could use our method to deduce their accretion disc radii. This would contribute to constraints on the fundamental system parameters, such as orbital separation and mass ratio, which might otherwise be impossible to determine.

## ACKNOWLEDGMENTS

We thank Andrew King for comments on an earlier version of this work. CRP was supported by a PPARC studentship, and thanks the OU Dept. of Physics and Astronomy for funding during the final write-up of this paper. MF acknowledges the CNRS for financial support. This research has made use of data obtained through the High Energy Astrophysics Science Archive Research Center Online Service, provided by NASA’s Goddard Space Flight Center (GSFC). ASM results were provided by the ASM and RXTE teams at MIT and at the RXTE SOF and GOF at NASA’s GSFC.

## REFERENCES

- Burderi L., King A. R., Szuszkiewicz E., 1998, *ApJ*, 509, 85  
 Campana S., Ravasio M., Israel G. L., Mangano V., Belloni T., 2003, *ApJ*, 594, L39  
 Chakrabarty D., Morgan E. H., 1998, *Nat*, 394, 346  
 Falanga M. et al., 2005, *A&A*, 436, 647  
 Foulkes S. B., Haswell C. A., Murray J. R., 2006, *MNRAS*, 366, 1399  
 Galloway D. K., Chakrabarty D., Morgan E. H., Remillard R. A., 2002, *ApJ*, 576, L137  
 Gierliński M., Poutanen J., 2005, *MNRAS*, 359, 1261  
 Haberl F., Titarchuk L., 1995, *A&A*, 299, 414  
 Hynes R. I. et al. 1998, *MNRAS*, 300, 64  
 Hynes R. I., Steeghs D., Casares J., Charles P. A., O’Brien K., 2004, *ApJ*, 609, 317  
 de Jong J. A., van Paradijs J., Augusteyn T., 1996, *A&A*, 314, 484  
 King A. R., Ritter H., 1998, *MNRAS*, 293, L42 (KR)  
 King A. R., 1998, *MNRAS*, 296, L45  
 Markwardt C. B., Swank J. H., Strohmayer T. E., in ‘t Zand J. J., Marshall F. E. 2002, *ApJ*, 575, L21  
 Nishiuchi M. et al., 1999, *ApJ*, 517, 436  
 Orosz J. A., Bailyn C. D., 1997, *ApJ*, 477, 876  
 Orosz J. A., Jain R. K., Bailyn C. D., McClintock J. E., Remillard R. A., 1998, *ApJ*, 499, 375  
 Orosz J. A. et al., 2002, *ApJ*, 568, 845  
 Park S. Q. et al., 2004, *ApJ*, 610, 378  
 Pringle J. E., 1981, *ARA&A*, 19, 137  
 Pringle J. E., 1996, *MNRAS*, 281, 357  
 Rappaport S., Joss P. C., 1997, *ApJ*, 486, 435  
 Shahbaz T., Charles P. A., King A. R., 1998, *MNRAS*, 301, 382 (SCK)  
 Trudolyubov S., Priedhorsky W., Cordova F., 2006, *ApJ*, 645, 277  
 in ‘t Zand J. J. M. et al., 2001, *A&A*, 372, 916